

Lattice Boltzmann Numerical Scheme for the Simulation of Natural Convection in an Inclined Square Cavity

*C. S. NOR AZWADI

Department of Thermo-fluid
Universiti Teknologi Malaysia
81310 UTM Skudai, Johor
MALAYSIA

azwadi@fkm.utm.my <http://www.fkm.utm.my/~azwadi>

N. I. NIK IZUAL

Faculty of Mechanical Engineering
Universiti Malaysia Pahang
26300 Kuantan Pahang
MALAYSIA

izual@ump.edu.my

Abstract: - In this paper, a mesoscale numerical method was applied to solve two dimensional, incompressible, thermal fluid flow problem. This study presents numerical prediction of natural convection heat transfer inside an inclined square cavity with perfectly conducting boundary conditions for the top and bottom walls. The lattice Boltzmann scheme with uniform mesh resolution was applied as a numerical research tool. The inclination angles were varied from 20° to 160° with 20° intervals. The results were presented in terms of streamlines and isotherms plots, and average Nusselt number in the system. We found that the flow structure together with the heat transfer mechanism are significantly dependence on the magnitude of the inclination angles. Good agreements were obtained when compared with the results published by other researchers in previous studies.

Key-Words: - Double population, lattice Boltzmann, distribution function, BGK collision, natural convection

1 Introduction

Flow in an enclosure driven by buoyancy force is a fundamental problem in fluid mechanics. This type of flow can be found in certain engineering applications within electronic cooling technologies, in everyday situation such as roof ventilation or in academic research where it may be used as a benchmark problem for testing newly developed numerical methods. A classic example is the case where the flow is induced by differentially heated walls of the cavity boundaries. Two vertical walls with constant hot and cold temperature is the most well defined geometry and was studied extensively in the literature. A comprehensive review was presented by David[1]. Other examples are the work by Azwadi and Tanahashi[2], Davis[3], Tric[4], Abdelhadi[5] and Sohrab[6].

The analysis of flow and heat transfer in a differentially heated side walls was extended to the inclusion of enclosure's inclination to the direction of gravity by Rasoul and Prinos[7]. This study performed numerical investigations into two-dimensional thermal fluid flows which are induced by the buoyancy force when the two facing sides of the cavity are heated to different temperatures. The cavity was inclined at angles from 40° to 160° , Rayleigh numbers from 10^3 to 10^6 and Prandtl numbers from 0.02 to 4000. Their results indicated that the mean and local heat flux at the hot wall

were significantly depend on the inclination angle. They also found that this dependence becomes stronger for the inclination angle greater than 90° .

Hart[8] performed a theoretical and experimental study of thermal fluid flow in a rectangular cavity at small aspect ratio and investigated the stability of the flow inside the system. Ozoe et al [9] conducted numerical analysis using finite different method on two-dimensional natural circulation in four types of rectangular cavity at inclination angles from 0° to 180° . Kuyper et al[10] provided a wide range of numerical predictions of flow in an inclined square cavity, covered from laminar to turbulent regions of the flow behavior. They applied $k-\varepsilon$ turbulence model and performed detailed analysis for Rayleigh numbers from 10^6 to 10^{10} .

A review of the available literatures shows that the flow behavior and heat transfer in a square cavity with the effect of Neumann typed boundary condition have not been discussed by previous researchers. The type of boundary condition applied on the bottom and top boundaries of the cavity strongly affects the heat transfer mechanism in the system[11][12]. Therefore, it is the purpose of present study to investigate the fluid flow behavior and heat transfer mechanism in an inclined square cavity, differentially heated sidewalls and perfectly conducting boundary condition for top and bottom walls.

Currently, numerical solutions to the fluid flow problem can be divided into three scales which are macro, meso and microscale solutions. Macroscale solution considers the Navier-Stokes equation as its governing equation and applies one or a combination of discretization methods to be solved using digital computer. However, due to the nonlinear nature of the equation, greater attention has to be paid during preprocessor step to determine suitable mesh size, criteria of computational stability, error propagation, etc.

There are few numerical solutions that simulate the evolution of fluid flow at microscopic scale. Among them are direct simulation Monte Carlo[13] and Molecular Dynamics method[14]. In these methods, the trajectories of every particle together with their position in the system are predicted using the second Newton's law. But remember, a cup of water contains 10^{23} number of molecules. Even when a gas is being considered where there are fewer molecules and a larger time-step can be used, because of the longer mean free path of the molecules, the number of molecules that can be considered is still limited. However, the question is do we really need to know the behavior of each molecule or atom? The answer is no. It is not important to know the behavior of each particle, it is important to know the function that can represent the behavior of many particles (mesoscale). Therefore, in current study, we bring the so-called lattice Boltzmann method to analyses the case in hand. The evolution of two distribution functions is considered to predict the velocity and temperature fields in the system. After showing how the formulation of mesoscale particle fits in to the framework of lattice Boltzmann simulations, a mathematical formulation is developed in order to investigate the effect of buoyancy force and inclination angle on the flow within the solution manifold.

The current study is summarized as follow: two-dimensional fluid flow and heat transfer in an inclined square cavity is investigated numerically. The two sidewalls are maintained at different temperatures while the top and bottom wall are set as a perfectly conducting wall. In current study, we fix the aspect ratio to unity. The flow structures and heat transfer mechanism are highly dependent upon the inclination angle of the cavity. By also adopting the Rayleigh number as a continuation parameter, the flow structure and heat transfers mechanism represented by the streamlines and isotherms lines can be identified as function of inclination angle. The computed average Nusselt number is also plotted to demonstrate the effect of inclination on

the thermal behavior in the system. Section two of this paper presents the governing equations for the case study in hand and introduces the numerical method which will be adopted for its solution. Meanwhile section three presents the computed results and provide a detailed discussion. The final section of this paper concludes the current study.

2 Governing Equations and Numerical Method

The physical domain of the problem is represented in Fig. 1. The flow is induced by the buoyancy force resulting from the constant heating of the right wall.

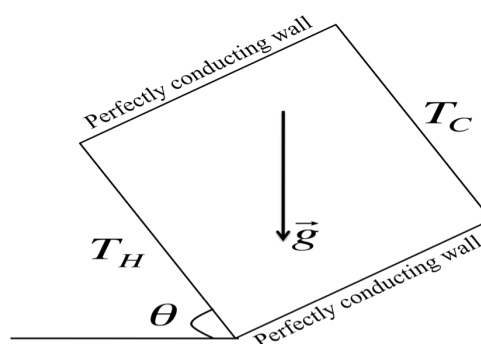


Fig. 1 Configuration of an inclined differentially heated enclosure's walls.

The system consists of a square enclosure with sides of length L and the hot wall is inclined at an angle of θ with the horizontal axis. The wall opposite to the hot wall is maintained at cold temperature while the other two walls are set at perfectly conducting boundary condition defined as

$$T = T_H - \left(\frac{x}{L}\right)(T_H - T_C) \quad (1)$$

There are two dimensionless parameters which govern the characteristic of thermal and fluid flow in the enclosure; the Prandtl and Rayleigh numbers defined as follow

$$Pr = \frac{\nu}{\chi} \quad (2)$$

$$Ra = \frac{g\beta(T_H - T_C)L^3}{\nu\chi}$$

In present study, the Prandtl number of 0.71 was used to represent the circulation of air in the system. The Rayleigh number is set at 10^5 . The Boussinesq approximation was included in the buoyancy force term so that all densities are assumed constant in the

body force term except the one in the gravity term which changes with temperature. Therefore, the body force term in x and y directions becomes

$$\begin{aligned} G_x &= \beta g(T - T_{ave}) \mathbf{j} \\ G_y &= \beta g(T - T_{ave}) \mathbf{i} \end{aligned} \quad (3)$$

The governing equations of the case in hand are the continuity, two-dimensional Navier Stokes and the energy equations. All of these equations are solved indirectly using the mesoscale numerical method of the lattice Boltzmann scheme. Two types of the evolution of particle distribution function [15][16][17] are brought to predict the density, velocity and temperature fields in the system. In the lattice Boltzmann scheme, it considers a fluid as an ensemble of artificial particles and explores the mesoscopic features of the fluid by using the propagation and collision effects among these particles. LBM discretizes the whole flow region into a number of grids and numerically solves the simplified Boltzmann equation on the regular lattices[18]. The solution to the lattice Boltzmann equation converged to the Navier-Stokes solution in continuum limit up to second order accuracy in space and time[19]. This method bridges the gap between the mesoscopic world and the macroscopic phenomena. LBM has emerged as a versatile numerical method for simulating various types of fluid flow problem including turbulent[20], multiphase[21], magnetohydrodynamics[22], flow in porous media[23], microchannel flow[24], etc.

The two distribution functions thermal lattice Boltzmann model starts with the evolution function and can be written as

$$f_i(\mathbf{x} + \mathbf{c}_i \Delta t, t + \Delta t) - f_i(\mathbf{x}, t) = -\frac{f_i - f_i^{eq}}{\tau_f} + F \quad (4)$$

$$g_i(\mathbf{x} + \mathbf{c}_i \Delta t, t + \Delta t) - g_i(\mathbf{x}, t) = -\frac{g_i - g_i^{eq}}{\tau_g} \quad (5)$$

where f_i^{eq} and g_i^{eq} are the density and temperature equilibrium distribution functions, respectively. c_i is the lattice velocity and i is the lattice direction, Δt is the time interval, τ_f and τ_g are the relaxation times of the density and temperature distribution functions, respectively. In LBM, the magnitude of c_i is set up so that in each time step Δt , the distribution function propagates in a distance of lattice nodes spacing Δx . This will ensure that the distribution function arrives exactly at the lattice nodes after Δt and collides simultaneously. The macroscopic variables such as

the density ρ , fluid velocity \mathbf{u} and temperature T can be computed in terms of the particle distribution functions as

$$\begin{aligned} \rho &= \int f \mathbf{c} \\ \rho \mathbf{u} &= \int \mathbf{c} f \mathbf{c} \\ T &= \int g \mathbf{c} \end{aligned} \quad (6)$$

To simulate the flow and thermal processes of the fluid in a system, one uses the D2Q9 model[25] with nine velocities assigned on a two-dimensional square lattice. These velocities include eight moving velocities along the links connecting the lattice nodes of the square lattice and a zero velocity for the rest particle. The rest of the particles is defined by the distribution functions f_0 , the particles moving in the orthogonal direction by the function f_i ($i = 1, 2, 3, 4$) and the particles moving in the diagonal directions by the function f_i ($i = 5, 6, 7, 8$)

The equilibrium distribution functions f_i^{eq} and g_i^{eq} are given as

$$f_i^{eq} = \rho \omega_i \left[1 + 3\mathbf{c}_i \cdot \mathbf{u} + 4.5(\mathbf{c}_i \cdot \mathbf{u})^2 - 1.5\mathbf{u}^2 \right] \quad (7)$$

$$g_i^{eq} = T \omega_i \left[1 + 3\mathbf{c}_i \cdot \mathbf{u} + 4.5(\mathbf{c}_i \cdot \mathbf{u})^2 - 1.5\mathbf{u}^2 \right] \quad (8)$$

where ω is the weight function and depends on the direction of the lattice velocity.

We next demonstrate the procedure to non-dimensionalize the lattice Boltzmann equations (Eqs. (4) and (5)). To do this, we define the reference parameters as follow

- Characteristic length scale, L
- Reference speed, U
- Reference density, n_r
- Time between particle collision, t_c

The dimensionless lattice Boltzmann equation can be written as

$$\hat{f}_i(\hat{\mathbf{x}} + \hat{\mathbf{c}}_i \Delta \hat{t}, \hat{t} + \Delta \hat{t}) - \hat{f}_i(\hat{\mathbf{x}}, \hat{t}) = -\frac{\hat{f}_i(\hat{\mathbf{x}}, \hat{t}) - \hat{f}_i^{eq}(\hat{\mathbf{x}}, \hat{t})}{\hat{\tau}_f \varepsilon} \quad (10)$$

where $\hat{\mathbf{c}} = \mathbf{c}/U$, $\hat{\mathbf{x}} = \mathbf{x}/L$, $\hat{t} = tU/L$, $\hat{f} = f/n_r$, $\Delta \hat{t} = \Delta t U/L$ and $\hat{\tau} = \tau/t_c$. The parameter $\varepsilon = t_c U/L$ can be interpreted as either the ratio of collision

time to flow time or as the ratio of mean free path to the characteristic length. The same procedure can be applied to obtain the dimensionless form of temperature distribution function. For simplification, all carets will be dropped and any terms referred to later are understood in dimensionless form.

Through a multiscaling, the mass and momentum equations can be derived from the evolution equation of Eq. (4). To see this, we first apply the Taylor series expansion of Eq. (4) and retaining terms up to second order gives

$$(\partial_t + \nabla \cdot \mathbf{c}_i) f_i + \frac{1}{2} (\partial_t^2 + 2\partial_t \nabla \cdot \mathbf{c}_i + \nabla \nabla : \mathbf{c}_i \mathbf{c}_i) f_i \quad (11)$$

In order to relate lattice Boltzmann equation with a macroscopic equation, it is necessary to separate different time scale. This is to indicate different scale of physical phenomena and contribute separately in the final macroscopic equation. To do this, space and time derivation are expanded in terms of Knudsen number ε as follow [25,26]

$$\partial_t = \varepsilon \partial_{t1} + \varepsilon^2 \partial_{t2} + O(\varepsilon^3) \quad (12)$$

$$\nabla = \varepsilon \nabla + O(\varepsilon^2) \quad (13)$$

Distribution function f_i is expanded about f_i^{eq} gives

$$f_i = f_i^{eq} + \varepsilon f_i^1 + \varepsilon^2 f_i^2 + O(\varepsilon^3) \quad (14)$$

where

$$\sum_i f_i^n = \sum_i \mathbf{c}_i f_i^n = 0 \text{ for } n \geq 1 \quad (15)$$

Eq. (15) implies that the non-equilibrium distribution function f_i^n does not contribute to the local values of density and momentum.

Substituting Eq. (12), (13) and (14) into (4) and regroup the equation to the first order of ε gives

$$(\partial_{t1} + \mathbf{c}_i \cdot \nabla) f_i^{eq} = -\frac{1}{\tau_f} f_i^1 \quad (16)$$

The equation to order ε^2 is simplified by using Eq. (15) gives

$$\partial_{t2} f_i^{eq} + (\partial_{t1} + \mathbf{c}_i \cdot \nabla) \left(1 - \frac{1}{2\tau_f} \right) f_i^1 = -\frac{1}{\tau_f} f_i^2 \quad (17)$$

A summation of Eq. (17) with respect to i is taken to give the first order of continuity equation

$$\partial_{t1} \rho + \nabla \cdot (\rho \mathbf{u}) = 0 \quad (18)$$

Next, multiplying Eq. (5) by \mathbf{c}_i and taking the summation as above leads to

$$\partial_{t1} (\rho \mathbf{u}) + \nabla \cdot \Pi^{eq} = 0 \quad (19)$$

where

$$\Pi^{eq} = \sum_i (\mathbf{c}_i \mathbf{c}_i) f_i \quad (20)$$

is the momentum flux tensor. After some simple mathematics manipulation to satisfy Galilean invariance and isotropic of tensor, the final expression for Π^{eq} is

$$\Pi^{eq} = c_s^2 \rho \delta_{\alpha\beta} + \rho u_\alpha u_\beta \quad (21)$$

Substituting Eq. (34) into Eq. (32) results in

$$\partial_{t1} (\rho \mathbf{u}) + \nabla \cdot (\rho \mathbf{u} \mathbf{u}) = -\nabla \cdot (c_s^2 \rho) \quad (22)$$

Eqs. (18) and (22) are known as Euler equation and the pressure is given by

$$p = c_s^2 \rho \quad (23)$$

Similarly, the equation for ρ and \mathbf{u} can be obtained from equation of ε^2 . Taking summation with respect to i of Eq. (17) gives

$$\partial_{t2} \rho = 0 \quad (24)$$

Multiplying Eq. (17) by \mathbf{c}_i and taking the summation as above gives

$$\partial_{t2} (\rho \mathbf{u}) + \nabla \cdot \left(1 - \frac{1}{2\tau_f} \right) \Pi^1 = 0 \quad (25)$$

where

$$\begin{aligned} \Pi^1 = & -\tau_f \left\{ \left(\frac{1}{3} - c_s^2 \right) \partial_\alpha (\rho u_\alpha) \delta_{\beta\gamma} + \frac{1}{3} \partial_\beta (\rho u_\gamma) \right. \\ & + \frac{1}{3} \partial_\gamma (\rho u_\beta) - u_\beta \partial_\gamma (c_s^2 \rho) - u_\gamma \partial_\beta (c_s^2 \rho) \\ & \left. - \partial_\alpha (\rho u_\beta u_\gamma u_\alpha) \right\} \end{aligned} \quad (26)$$

Combining equations of $O(\varepsilon)$ and $O(\varepsilon^2)$ gives the correct form of the continuity equation

$$\nabla \cdot \mathbf{u} = 0 \quad (27)$$

and the momentum equation for an incompressible fluid

$$\partial_t (\rho u_\alpha) + \partial_\gamma (\rho u_\alpha u_\beta) = -\partial_\alpha (c_s^2 \rho) + \partial_\beta \left(2\rho \frac{2\tau_f - 1}{6} S_{\alpha\beta} \right) \quad (28)$$

where $S_{\alpha\beta} = \frac{1}{2} (\partial_\alpha u_\beta + \partial_\beta u_\alpha)$, $p = c_s^2 \rho$ and the sound speed is given by

$$c_s^2 = \frac{1}{3} \quad (29)$$

From above derivations, we can see that the evolution equation of distribution function can lead to the incompressible Navier-Stokes equation through Chapman-Enskog expansion.

It is well known that for the prediction at low and moderate Rayleigh numbers, the viscous heat dissipation and compression work carried out by the pressure are negligible. The temperature field is then passively advected by the fluid flow and obeys a simpler passive-scalar equation

$$\frac{\partial T}{\partial t} + \nabla \cdot (\mathbf{u}T) = \chi \nabla^2 T \quad (30)$$

The detailed derivation of (30) from the D2Q9 model of the temperature distribution function can be seen in Azwadi and Tanahashi[27]. The time relaxations τ_f and τ_g in mesoscopic world can be related to the viscosity and diffusivity in the macroscopic world as follow

$$\begin{aligned} \tau_f &= 3\nu + 0.5 \\ \tau_g &= 3\chi + 0.5 \end{aligned} \quad (31)$$

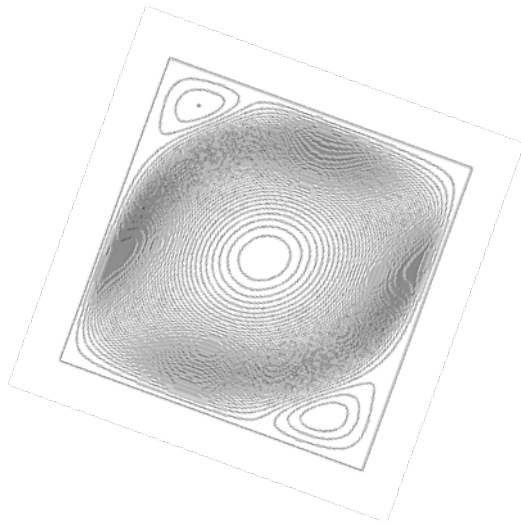
4 Results and Discussion

In the previous section, we have set up the physical problem and the calculation domain. We then derived the mathematical model to solve the natural convection problem in an inclined cavity and proceed with the choice of numerical method.

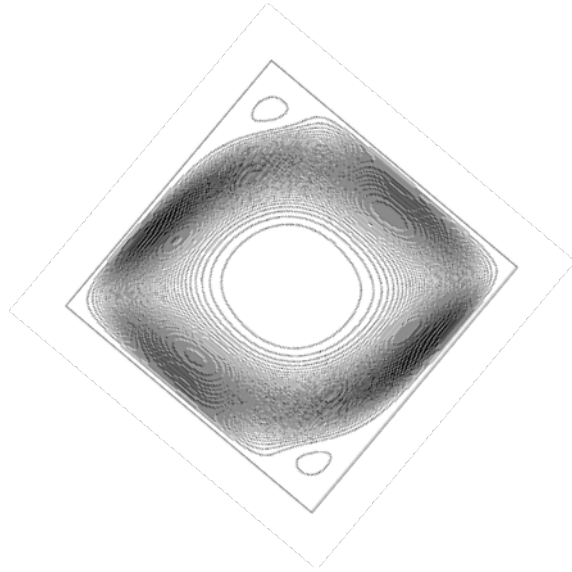
In this section, the predicted numerical results will be discussed in terms of streamlines and isotherms plots. Fig. 2 shows the plots of streamline for inclination angles from 20° to 160° . As can be seen from the figure, for the simulation at high inclination angle ($\theta \geq 60^\circ$), boundary layers are formed along the hot and cold walls. The air near the hot wall is heated and goes up due to the buoyancy effect before it hits the corner with the perfectly conducting walls and spread to a wide top wall. Then as it is cooled by the cold wall, the air gets heavier and goes downwards to complete the cycle.

At low value of inclination angle ($\theta \geq 20^\circ$), two small vortices are formed at the upper corner and lower corner of the enclosure indicates high magnitude of flow velocity near these regions. The presence of these two corner vortices compressed the central cell to form an elongated vortex. The isotherms show a good mixing occurring in the center and relatively small gradient indicating small value of the local Nusselt number along the differentially heated walls.

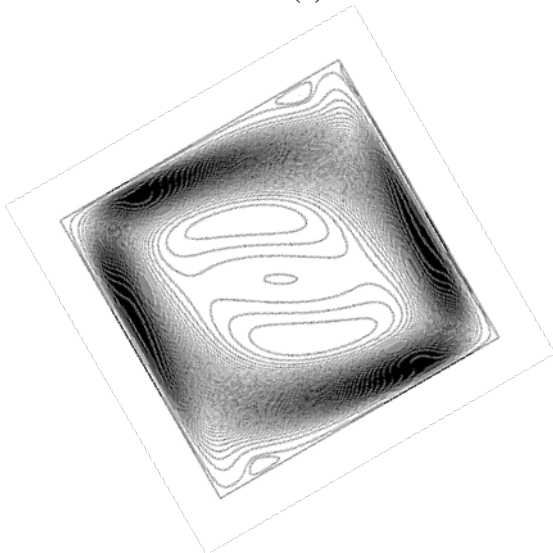
Further increment of inclination angle ($\theta = 40^\circ$) leads to the size reduction of small corner vortices. At $\theta = 60^\circ$, the small corner vortices completely disappear and the central cell pointing towards the corners because high magnitude of gravity vector drag the outer vortex along the vertical walls of the enclosure. Denser isotherms lines can be seen from the figure indicates higher value of local and average Nusselt number compared to previous inclination angles. Further inclination of enclosure separates the main central vortex into two smaller vortices. As we increase the inclination angle, these two vortices grow in size indicates that some fluid from the hot or cold wall returns back to the same wall. For inclination angles of $\theta = 80^\circ$ to $\theta = 120^\circ$, the isotherms line are parallel to the perfectly conducting walls indicates that the main heat transfer mechanism is by convection. Denser isotherms lines can be seen near the bottom left and top right corners demonstrates high local Nusselt number near these regions. However, at high inclination angles ($\theta \geq 140^\circ$), the isotherms lines are equally spaced indicates low averages Nusselt number in the system.



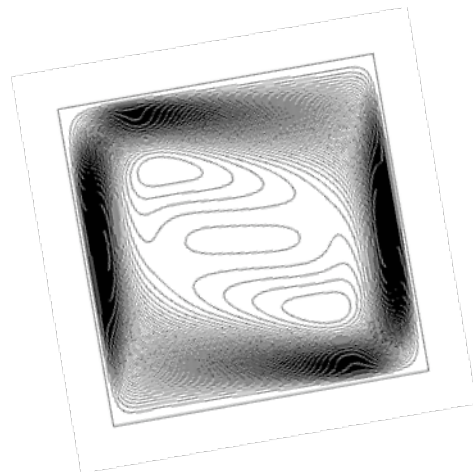
(a) $\theta = 20^\circ$



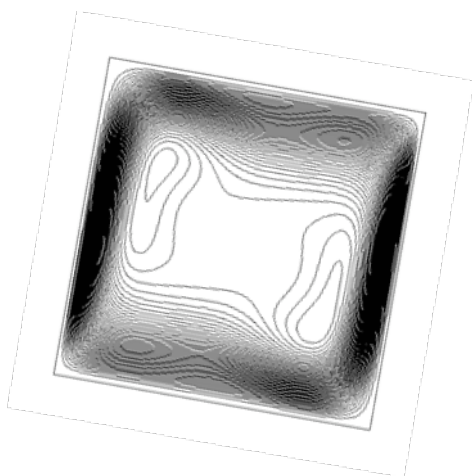
(b) $\theta = 40^\circ$



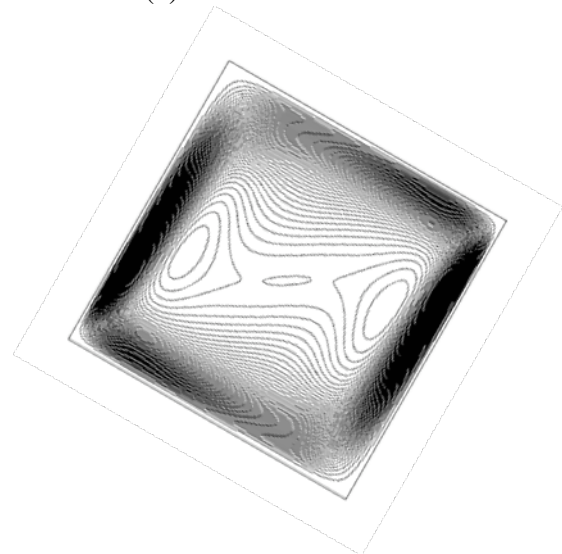
(c) $\theta = 60^\circ$



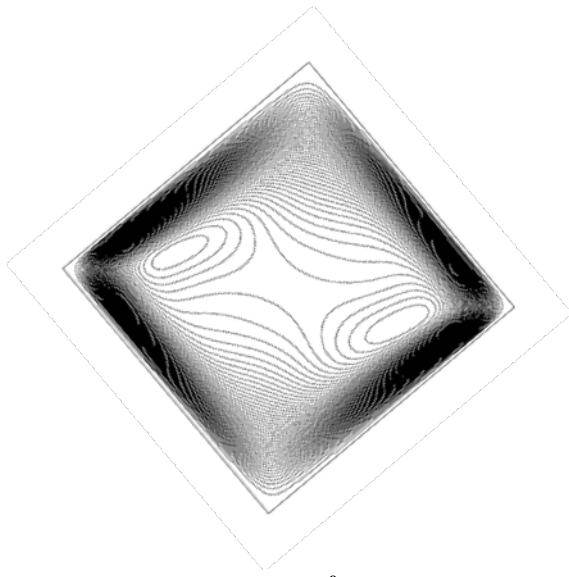
(d) $\theta = 80^\circ$



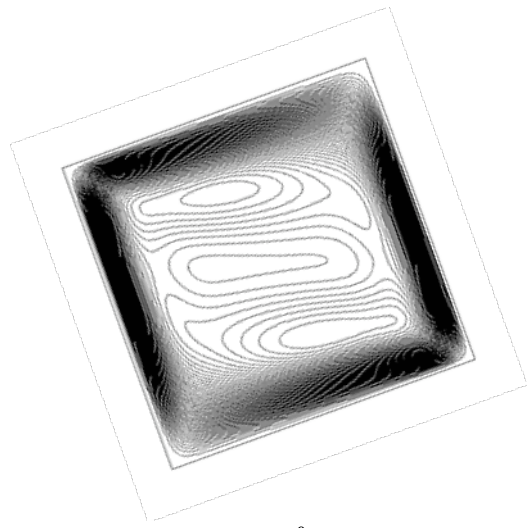
(e) $\theta = 100^\circ$



(f) $\theta = 120^\circ$

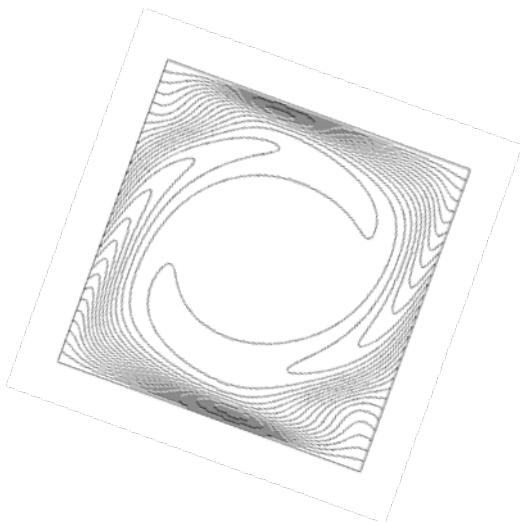


(g) $\theta = 140^\circ$

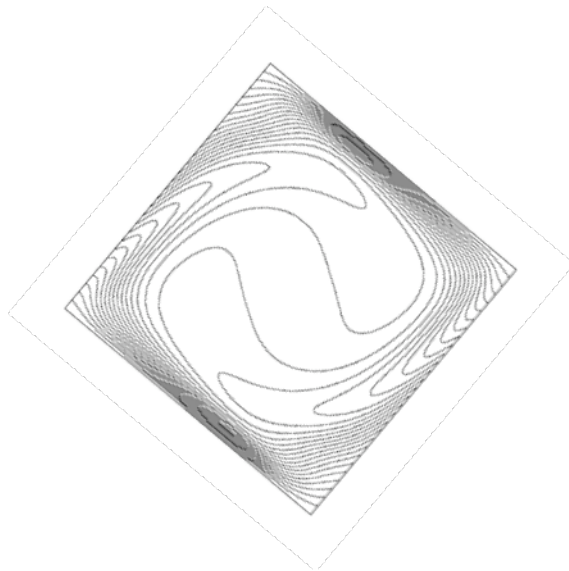


(h) $\theta = 160^\circ$

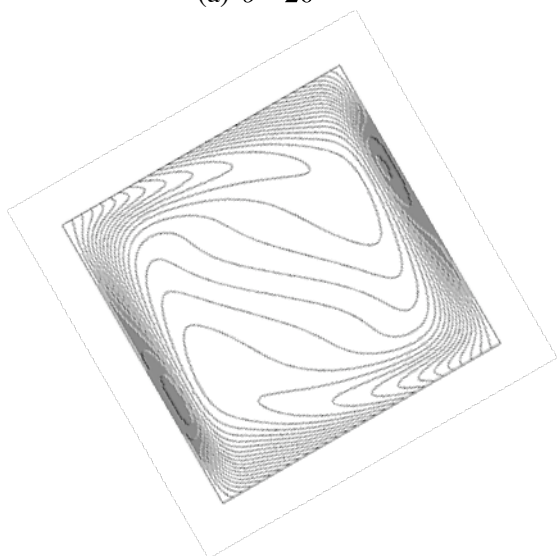
Fig. 2 Streamlines plots for every inclination angle.



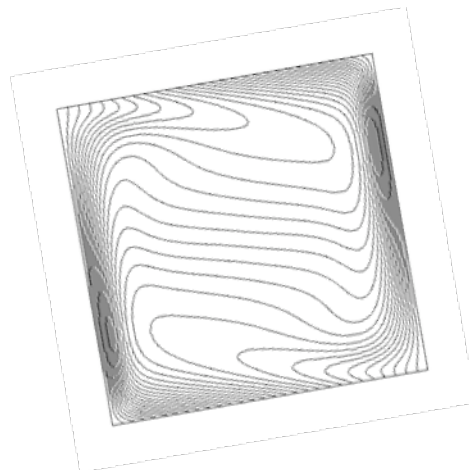
(a) $\theta = 20^\circ$



(b) $\theta = 40^\circ$



(c) $\theta = 60^\circ$



(d) $\theta = 80^\circ$

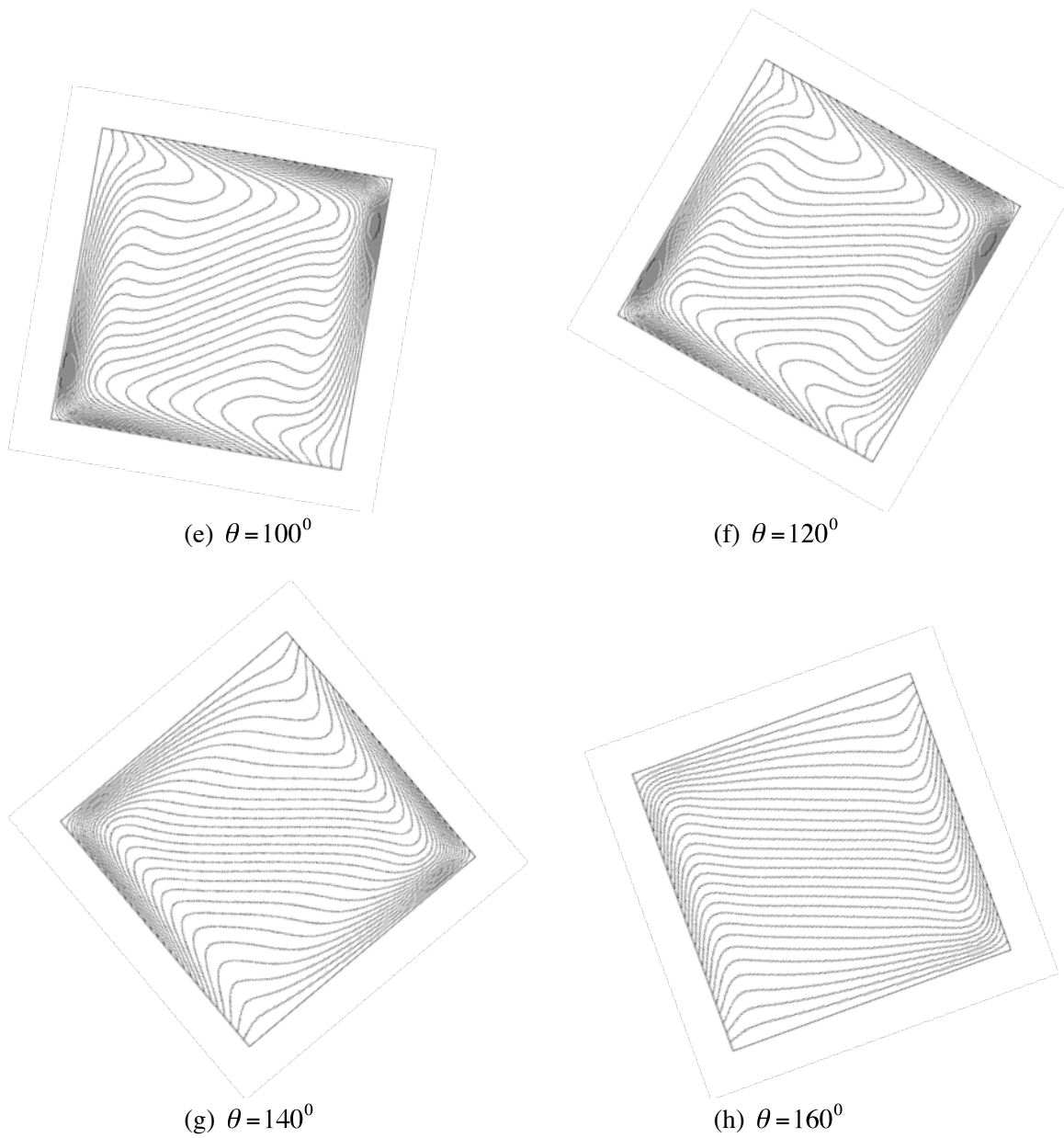


Fig. 3 Isotherms plots for every inclination angle.

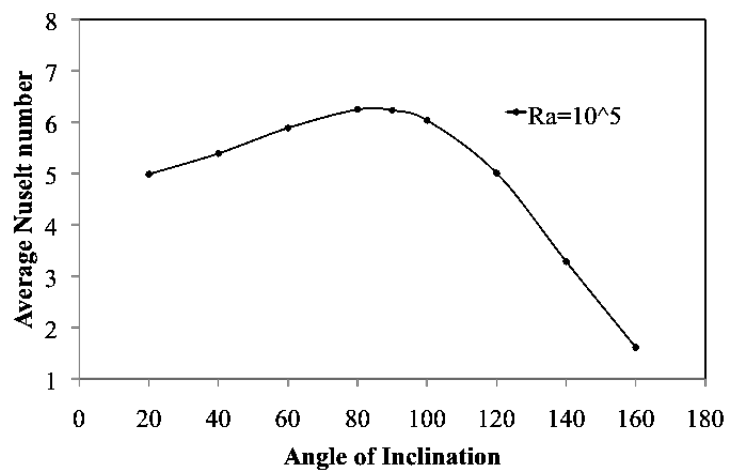


Fig. 4 Effect of inclination angles on average Nusselt number

The effect of the inclination angle on the average Nusselt number is shown in Fig. 4. For all simulated cases, the computed Nusselt numbers are lower than those for the case of adiabatic types of boundary condition[7] because the heat is allowed to pass through the top and bottom walls. The maximum value of average Nusselt number is determined at inclination angle between 80° to 100° . These can be explained by analyzing the isotherms plots which demonstrating relatively denser lines near hot and cold walls leading to high temperature gradient near these regions. Lower value of average Nusselt number at lower inclination angle was due to the presence of small corner vortices which contributes smaller local heat transfer along the hot and cold walls.

For the computation at higher inclination angles, where the hot wall is close to the top position, the magnitude of the gravity vector is reduced results in low magnitude of flow velocity along the hot wall. Due to this reason, the heat transfer rates are small resulted from the reduction in the driving potential for free convection. All of these phenomena are in good agreement with previous reported studies[7][8][9][10].

5 Conclusion

The natural convection in an inclined cavity has been simulated using the mesoscale numerical scheme where the Navier Stokes equation was solved indirectly using the lattice Boltzmann method. The result of streamlines plots clearly depicting the flow pattern and vortex structure in the cavity. The primary vortex is transformed from a double cellular to a single cellular as the inclination angle decreases. These demonstrate the lattice Boltzmann numerical scheme the passive-scalar thermal lattice Boltzmann model is a very efficient numerical method to study flow and heat transfer in a differentially heated inclined enclosure.

Acknowledgement

The authors would like to thank Universiti Teknologi Malaysia and Malaysia government for supporting these research activities. This research was conducted under FRGS research grant, vot 78340.

References:

- [1] H.O. Patrick and N. David, *Introduction to Convective Heat Transfer Analysis*, McGraw Hill, 1999.
- [2] C.S Nor Azwadi and T. Tanahashi, Simplified Thermal Lattice Boltzmann in Incompressible Limit, *International Journal of Modern Physics B*, Vol.20, No.17, 2006, pp. 2437-2449.
- [3] D.V. Davis, Natural Convection of Air in a Square Cavity; A Benchmark Numerical Solution, *International Journal for Numerical Methods in Fluids*, Vol.3, No.3, 1983, pp. 249-264.
- [4] E. Tric, G. Labrosse and M. Betrouni, A First Incursion into the 3D Structure of Natural Convection of Air in a Differentially Heated Cubic Cavity, from Accurate Numerical Solutions, *International Journal of Heat and Mass Transfer*, Vol.43, No.21, 2000, pp. 4043-4056.
- [5] B. Abdelhadi, G. Hamza, B. Razik and E. Raouache, Natural Convection and Turbulent Instability in Cavity, *WSEAS Transactions on Heat and Mass Transfer*, Vol.1, No.2, 2006, pp. 179-184.
- [6] S.H. Sohrab, A Modified Theory of Laminar Flow by Free Convection on a Vertical Hot Surface, *WSEAS Transactions on Biology and Biomedicine*, Vol.2, No.2, 2005, pp. 192-198.
- [7] Rasoul and Prinos, Natural Convection in an Inclined Enclosure, *International Journal of Numerical Methods for Heat and Fluid Flow*, Vol.7, No.5, 1997, pp. 438-478.
- [8] J.E. Hart, Stability of the Flow in a Differentially Heated Inclined Box, *Journal of Fluid Mechanics*, Vol.47, No.3, 1971, pp.547-576.
- [9] H. Ozoe, K. Yamamoto, H. Sayama and W.C. Stuart, Natural Circulation in an Inclined Rectangular Channel Heated on One Side and Cooled on the Opposing Side, *International Journal of Heat and Mass Transfer*, Vol.17, No.10, 1974, pp.1209-1217.
- [10] R.A. Kuyper, T.H. Van Der Meer, C.J. Hoogendoorn and R.A.W.M. Henkes, Numerical Study of Laminar and Turbulent Natural Convection in an Inclined Square Cavity, *International Journal of Heat and Mass Transfer*, Vol.36, No.11, 1993, pp.2899-2911.
- [11] C.S Nor Azwadi, M.F.M. Yasin and S. Samion, Virtual Study of Natural Convection Heat Transfer in an Inclined Square Cavity, *Journal of Applied Science*, Vol. 10, No.3, 2010, pp.331-336.

- [12] M. Paroncini, F. Corvaro and M.M. Padova, Study and Analysis of the Influence of a Small Heating Source Positioned on the Natural Convective Heat Transfer in a Square Cavity, *WSEAS Transaction on Heat and Mass Transfer*, Vol.1, No.4, 2006, pp. 461-466.
- [13] G.A. Bird, Approach to Translational Equilibrium in a Rigid Sphere Gas, *Physics of Fluid*, Vol.9, 1963, pp.1518-1519.
- [14] B.J. Alder and T.E. Wainwright, Phase Transition for a Hard Sphere System, *Journal of Chemical Physics*, Vol.27, 1957, pp. 1207-1208.
- [15] X. He, S. Shan and G. Doolen, A Novel Thermal Model for Lattice Boltzmann Method in Incompressible Limit, *Journal of Computational Physics*, Vol.146, No.1, 1998, pp. 282-300.
- [16] C.S. Nor Azwadi and S. Syahrullail, A Three-Dimension Double-Population Thermal Lattice BGK Model for Simulation of Natural Convection Heat Transfer in a Cubic Cavity, *WSEAS Transaction on Mathematics*, Vol.8, No.9, 2009, pp. 561-571.
- [17] F. Nathan and H. Richard, Simulating Acoustic Propagation using a Lattice Boltzmann Model of Incompressible Fluid Flow, *WSEAS Transactions on Signal Processing*, Vol.2, No.6, 2006, pp. 876-881.
- [18] S. Hou, Q. Zou, S. Chen, G. Doolen and A. C. Cogley, Simulation of Cavity Flow by the Lattice Boltzmann Method, *Journal of Computational Physics*, Vol.118, No.2, 1995, pp. 329-347.
- [19] S. Chen and G. Doolen, Lattice Boltzmann Method for Fluid Flows, *Annual Review of Fluid Mechanics*, Vol.30, No.1, 1998, pp. 329-364.
- [20] L. Jonas, B. Chopard, S. Succi and F. Toschi, Numerical Analysis of the Average Flow Field in a Turbulent Lattice Boltzmann Simulation, *Physica A*, Vol.362, No.1, 2006, pp. 6-10.
- [21] S. Alapati, S. Kang and Y. K. Suh, 3D Lattice Boltzmann Simulation of Droplet Formation in a Cross-Junction Microchannel, *Proceeding of the 3rd IASME/WSEAS International Conference on Continuum Mechanics*, 2008.
- [22] G. Breyiannis and D. Valougeorgis, Lattice Kinetic Simulations in Three-Dimensional Magnetohydrodynamics, *Physical Review E*, Vol.69, No.6, 2004, pp. 065702/1-065702/4.
- [23] Z. Guo, Lattice Boltzmann Model for Incompressible Flows through Porous Media, *Physical Review E*, Vol.66, No.3, pp.036034/1-036034/9
- [24] Y. Zhang, R. Qin and D.R. Emerson, Lattice Boltzmann Simulation of Rarefied Gas Flow in Microchannel, *Physical Review E*, Vol.71, No.4, pp.047702/1-047702/4.
- [25] X. He and L.S. Luo, Lattice Boltzmann Model for the Incompressible Navier-Stokes Equation, *Journal of Statistical Physics*, Vol.88, No.3, 1997, pp. 927-944.
- [26] Y. Peng, C. Shu and Y.T. Chew, A 3D Incompressible Thermal Lattice Boltzmann Model and its Application to Simulation Natural Convection in a Cubic Cavity, *Journal of Computational Physics*, Vol.193, No.1, 2003, pp. 260-274.
- [27] C.S. Nor Azwadi and T. Tanahashi, Simplified Finite Difference Thermal Lattice Boltzmann Method, *International Journal of Modern Physics B*, Vol.22, No.22, 2008, pp. 3865-3876.
- [28] Y.H. Qian, D. Humieres and P. Lallemand, Lattice BGK for Navier-Stokes Equation, *Europhysics Letter*, Vol.17, No.6, 1992, pp. 479-484.